J. Am. Soc. Mass Spectrom. (2016) 27:542–551
DOI: 10.1007/s13361-015-1302-z

RESEARCH ARTICLE

Ambient Molecular Analysis of Biological Tissue Using Low-Energy, Femtosecond Laser Vaporization and Nanospray Postionization Mass Spectrometry

Fengjian Shi,[1,2] Paul M. Flanigan IV,[1,2,3]
Jieutonne J. Archer,[1,2] Robert J. Levis[1,2]

[1]Department of Chemistry, Temple University, 1901 N. 13th St., Philadelphia, PA 19122, USA
[2]Center for Advanced Photonics Research, Temple University, 1901 N. 13th St., Philadelphia, PA 19122, USA
[3]*Present Address:* Signature Science, LLC., 2819 Fire Rd, Egg Harbor Township, NJ 08234, USA

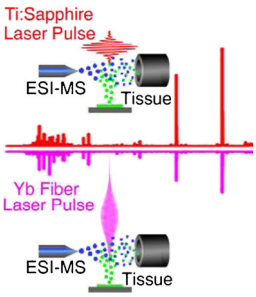

Abstract. Direct analysis of plant and animal tissue samples by laser electrospray mass spectrometry (LEMS) was investigated using low-energy, femtosecond duration laser vaporization at wavelengths of 800 and 1042 nm followed by nanospray postionization. Low-energy (<50 μJ), fiber-based 1042 nm LEMS (F-LEMS) allowed interrogation of the molecular species in fresh flower petal and leaf samples using 435 fs, 10 Hz bursts of 20 pulses from a Ytterbium-doped fiber laser and revealed comparable results to high energy (75–1120 μJ), 45 fs, 800 nm Ti:Sapphire-based LEMS (Ti:Sapphire-LEMS) measurements. Anthocyanins, sugars, and other metabolites were successfully detected and revealed the anticipated metabolite profile for the petal and leaf samples. Phospholipids, especially phosphatidylcholine, were identified from a fresh mouse brain section sample using Ti:Sapphire-LEMS without the application of matrix. These lipid features were suppressed in both the fiber-based and Ti:Sapphire-based LEMS measurements when the brain sample was prepared using the optimal cutting temperature compounds that are commonly used in animal tissue cryosections.

Keywords: Femtosecond fiber laser, Biological tissue, Ambient mass spectrometry, Laser vaporization, Electrospray ionization

Received: 12 August 2015/Revised: 22 October 2015/Accepted: 27 October 2015/Published Online: 14 December 2015

Introduction

The ability to detect biomolecules (e.g., small metabolites, lipids, and proteins) directly from biological samples remains one of the most important topics in molecular systems biology [1]. Numerous studies have demonstrated that the concentration and distribution of metabolites, such as hydrocarbons, sugars, amino acids, alkaloids, and lipids, are closely associated with biological processes in a living organism [2]. Label-assisted techniques such as fluorophore-tagging microscopy are usually used to characterize the biological samples, in vivo or ex vivo, and rely on labeling/staining methods that may perturb the biological system. Label-free techniques such as infrared [3] and Raman [4] spectroscopy can interrogate the sample with submicron lateral resolution in a noninvasive manner. However, such spectroscopy techniques rely upon the vibrational modes of the molecules in question, which require prior knowledge for interpretation, and lack chemical specificity for individual compounds. Mass spectrometry (MS), on the other hand, has seen rapid deployment in biological sample analysis because the requirements of high throughput, sensitivity, and specificity can be simultaneously satisfied in one measurement. In particular, the introduction of ambient ionization mass spectrometry allows analysis with minimal or no sample preparation under ambient conditions, thus preserving the native state of the sample [5, 6].

The goal of understanding complex biological systems, ranging from intact body [7] to tissue sections [8–12], to body fluids [13, 14], to single cells [15, 16], has been the driving force for the advent of various ambient ionization MS techniques in the last decade. Plasma-based techniques like direct analysis in real time (DART) or low temperature plasma (LTP)

Electronic supplementary material The online version of this article (doi:10.1007/s13361-015-1302-z) contains supplementary material, which is available to authorized users.

Correspondence to: Robert J. Levis; *e-mail:* rjlevis@temple.edu

are ideal for the analysis of volatile analytes [17, 18], and have been used to explore the hydrocarbon profile of live flies [7] as well as the metabolite distribution of a chili fruit [19]. Liquid extraction sampling techniques, including liquid microjunction surface sampling probe (LMJ-SSP) [8], liquid extraction surface analysis (LESA) [20], nanospray desorption ionization (nano-DESI) [21], and single-probe [16], are powerful tools to study the distribution of lipids, drugs, and metabolites in animal tissues [8, 20, 22], bacterial colonies [23], and single cells [16], but require careful design and optimization to manipulate the liquid sampling probe because of the physical and chemical heterogeneity of the sample in question. The spray-based technique desorption electrospray ionization (DESI) has high sensitivity, histologic compatibility, and lateral analysis capability [9, 24], but routine DESI has a spatial resolution of ~200 μm, although a resolution of 35 μm has been demonstrated through careful optimization of the spray operating parameters [25], and the analysis is limited to compounds that are ionized by ESI-like processes [5].

Methods that use laser desorption/electrospray ionization hybrid ambient ionization sources combine the microsampling capability of a laser beam with the high ionization efficiency of an electrospray source [26]. Several such techniques, electrospray-assisted laser desorption ionization (ELDI) [27], laser ablation electrospray ionization (LAESI) [13], infrared matrix-assisted laser desorption electrospray ionization (IR-MALDESI) [28], and laser electrospray mass spectrometry (LEMS) [29], can provide a lateral resolution of 20−200 μm without the necessity of adding external matrix to the sample. Different mechanisms have been proposed for the laser desorption step of these laser/electrospray hybrid techniques depending on the laser wavelength and pulse duration while they share similar ionization mechanism. LAESI and IR-MALDESI employ a nanosecond IR laser at a wavelength of 2.94 μm and take advantage of the inherent water present in many biological systems to absorb the energy required to induce desorption because water has a strong absorption band at the laser radiation wavelength [13, 28]. In LEMS, laser pulses as short as 60 fs, usually at 800 nm, interact with the analytes via a nonlinear, multiphoton excitation mechanism [29]. LEMS does not require either the analyte or matrix to be linearly resonant with the laser wavelength and shows little dependence on the types of sample substrate employed [30]. Various biological samples, including chicken egg albumen and yolk [31], reduced fat and whole milk [32], whole blood [31, 32], and plant samples [33, 34] have been successfully characterized by LEMS without the use of external matrix. Investigations of animal tissue samples, a popular target of MS imaging, have not been performed so far by LEMS to examine the feasibility of femtosecond laser vaporization for chemical analysis of animal tissue samples.

The nonresonant, multiphoton excitation process in LEMS occurs when the sample of interest is subjected to a femtosecond laser pulse at an intensity of 10^{13}–10^{14} W/cm^2, which is 6 to 7 orders of magnitude higher than a nanosecond UV or IR laser desorption source under the same laser pulse energy and focusing condition. A solid state Ti:Sapphire amplifier seeded by a Ti:Sapphire oscillator is usually used to create laser pulses at 800 nm with high pulse energy (μJ–mJ) and ultrashort pulse duration (40–60 fs) to fulfill the high intensity requirement. However, the higher cost and lower robustness of the Ti:Sapphire amplified femtosecond laser in comparison with the more common nanosecond UV and IR lasers limit the wide application of Ti:Sapphire laser as a desorption source. In recent studies, we successfully implemented a low-energy, femtosecond fiber laser for vaporization and a nanospray for postionization in the analysis of proteins, whole blood [35], and substituted benzylpyridinium salts [36]. The studies show that the low-energy fiber laser resulted in comparable internal energy distributions to nanospray [36] and retained intact biological macromolecules after laser radiation [35]. The application of a femtosecond fiber laser rather than a solid state amplifier laser to more complex biological samples is thus of interest for the broad and potential applicability of LEMS as a robust, portable, and affordable analytical tool to non-specialists.

Here, we extend the use of the fiber-based 1042 nm laser vaporization to the analysis of biological tissue samples and compare the results with Ti:Sapphire-based 800 nm laser measurements. A lipid standard sample, 1,2-dihexanoyl-*sn*-glycero-3-phosphocholine PC(6:0/6:0), is analyzed via fiber-based LEMS (F-LEMS) and Ti:Sapphire-based LEMS (Ti:Sapphire-LEMS). We investigate the vaporization of fresh Begonia flower petal and leaf samples using F-LEMS and Ti:Sapphire-LEMS. A mouse brain section is also characterized by the Ti:Sapphire laser without application of any external matrix. Finally, the effect of optimal cutting temperature (OCT) compounds on the analysis of mouse brain sections by F-LEMS and Ti:Sapphire-LEMS is investigated.

Experimental

Materials

The lipid standard sample PC(6:0/6:0) was purchased from Avanti Polar Lipids Inc. (Alabaster, AL, USA). HPLC grade methanol and water were purchased from Fisher Scientific (Fair Lawn, NJ, USA) and Burdick & Jackson (Muskegon, MI, USA), respectively. Glacial acetic acid was purchased from EMD Chemicals (Gibbstown, NJ, USA).

Sample Preparation

Stock solution of PC(6:0/6:0) was prepared in 1:1 (v:v) methanol:water solution at a concentration of 250 μM. For laser vaporization experiments, 15 μL aliquot of the lipid solution was deposited on a stainless steel sample slide and allowed to air-dry to a circular spot of ~5 mm in diameter. Fresh Begonia flower petal and leaf samples (insets of Figure 2a and c) were collected from plants on the Temple University campus. The flowers were harvested from different plants with 3~4 leaves attached and then separated to petal and leaf samples. The petal and

leaf samples were affixed to the stainless steel and glass sample slides using double-sided tape prior to analysis. The center regions of the petal or leaf samples were raster scanned and irradiated by laser during analysis. Fresh mouse brain samples were obtained from a healthy mouse and stored in PBS buffer (pH 7.4) with an ice bath. Prior to sectioning, the brain sample was wrapped in a piece of aluminum foil and flash frozen in liquid nitrogen. The frozen brain was then immediately cut into ~200 μm thick transverse sections by a stainless steel blade (X-ACTO #11; Statesville, NC, USA) over the liquid nitrogen under a microscope (Leica Zoom 2000; Buffalo Grove, IL, USA). The sections were thaw-mounted onto microscope slides (Fisher Scientific, Pittsburgh, PA, USA) and stored at −80°C. OCT-embedded mouse brain tissue cryosections (5 μm thickness) were obtained from Department of Pathology and Laboratory Medicine (Temple University, Philadelphia, PA, USA), mounted on the microscope slides and stored at −80°C. Fresh and OCT-embedded mouse brain section slides were brought to room temperature under atmospheric pressure in ~15 min prior to analysis. All animal procedures followed the Guide for the Care and Use of Laboratory Animals by NIH/NRC. The lipid, plant, and brain sample slides were then placed on the sample stage and subjected to laser vaporization without further treatment.

Laser Electrospray Mass Spectrometry

The experimental schemes of fiber-based and Ti:Sapphire-based LEMS source are shown in Figure 1. Laser vaporization for F-LEMS or Ti:Sapphire-LEMS was performed using a fiber-based femtosecond laser (μJewel DE series; IMRA America Inc., Ann Arbor, MI, USA) or a Ti:Sapphire-based femtosecond laser (Legend Elite HE series; Coherent Inc., Santa Clara, CA, USA), respectively. Both lasers were composed of an oscillator and an amplifier to produce amplified, high energy laser pulses (μJ to mJ). The fiber laser employs a Yb-doped fiber as the gain medium in the oscillator and amplifier cavity, employs single-mode fibers for directing the laser beam in and out the cavity, and is air-cooled rather than utilizing a chiller. All of these features provide a femtosecond fiber laser with a compact and robust design in comparison with the solid state Ti:Sapphire laser.

The laser vaporization source was described in detail previously for the Ti:Sapphire-LEMS [29] and has been recently modified to couple the fiber laser to the electrospray inlet of a quadrupole time of flight (QTOF) mass spectrometer (micrOTOF-Q II; Bruker Daltonik GmbH, Bremen, Germany) [35, 36]. Briefly, the fiber laser delivers 100 kHz, 435 fs, 1042 nm pulses with maximum pulse energy of 50 μJ. For laser desorption, the pulse repetition rate was stepped down to 10 Hz bursts of 20 pulses by combining a 20 Hz chopper and a 130 Hz chopper. The pulse energy was adjusted by a quarter-wave plate and a beam splitter cube from 20 μJ to 46.5 μJ. The Ti:Sapphire laser was operated at 10 Hz to create 45 fs, 800 nm laser pulses with maximum pulse energy of up to 5 mJ. The pulse energy was controlled by a pair of neutral density filters to be 75−1120 μJ for the purpose of laser desorption. The samples were placed on a copper sample stage, which was raster scanned by a two-dimensional microscopy stage (MLS203-1; Thorlabs, Newton, NJ, USA) below the nanospray source during laser vaporization. The attenuated laser pulses from the fiber laser or the Ti:Sapphire laser were focused onto the sample surface to a ~75 μm diameter spot with a 10 cm lens at 45° incident angle. The resulting intensities of field were approximately 2.39×10^{12} W/cm^2 and 3.77×10^{13} W/cm^2 when the pulse energy was 46.5 μJ and 75 μJ for the fiber laser and Ti:Sapphire laser, respectively.

The laser vaporized analytes were captured and postionized by a nanospray source. A solution containing 1:1 (v:v) methanol:water with 1% acetic acid was infused to a tapered silica emitter tip (50 μm i.d., 20 μm tip i.d.; New Objective, Woburn, MA, USA) at a flow rate of 250 nL/min using a syringe pump (Model 100; KD Scientific, Holliston, MA, USA). A stable positive mode nanospray mass spectrum was observed when the capillary inlet was biased to −2 kV and the needle was grounded. The sample stage was biased to −1.3 kV during laser vaporization. The spectrometer was calibrated by an ESI calibrant solution (63606; Fluka Analytical/Sigma-Aldrich, Buchs, Switzerland) over a mass range of *m/z* 50 −2000. The in-source collision region (ISCID) and collision cell (CID) voltages were set to be 0 and 10 eV, respectively. Raw mass spectra were acquired at a rate of 1 Hz by Bruker Compass micrOTOF control software (ver. 3.0; Bruker Daltonik GmbH, Bremen, Germany). A typical measurement was performed within 40 s per sample. Within this period, 10 blank spectra and 25 to 30 spectra of the sample were acquired. Each measurement was repeated at least two times for a total of 50 to 60 spectra per sample.

Data Analysis

The acquired mass spectra were processed in Bruker Compass DataAnalysis software (ver. 4.0 SP1; Bruker Daltonik GmbH, Bremen, Germany), including signal averaging, blank subtraction, and mass assignment. The processed spectra were exported and plotted in Origin 8.0 (OriginLab, Northampton, MA, USA). Peaks were labeled and confirmed by comparing the blank-subtracted spectra with the nanospray blank spectra. Features identified from plant sample were assigned by searching in the METLIN database [37] (http://metlin.scripps.edu/index.php, last accessed April 23, 2015) and Plant Metabolic Network (http://www.plantcyc.org/, last accessed April 23, 2015) with a maximum mass tolerance of 10 ppm. Identification of lipids from mouse brain sample were enabled by accurate lipids database search in METLIN [37] (http://metlin.scripps.edu/index.php, last accessed April 23, 2015) and LIPID MAPS [38] (http://www.lipidmaps.org/, last accessed April 23, 2015) with a tolerance of 20 ppm.

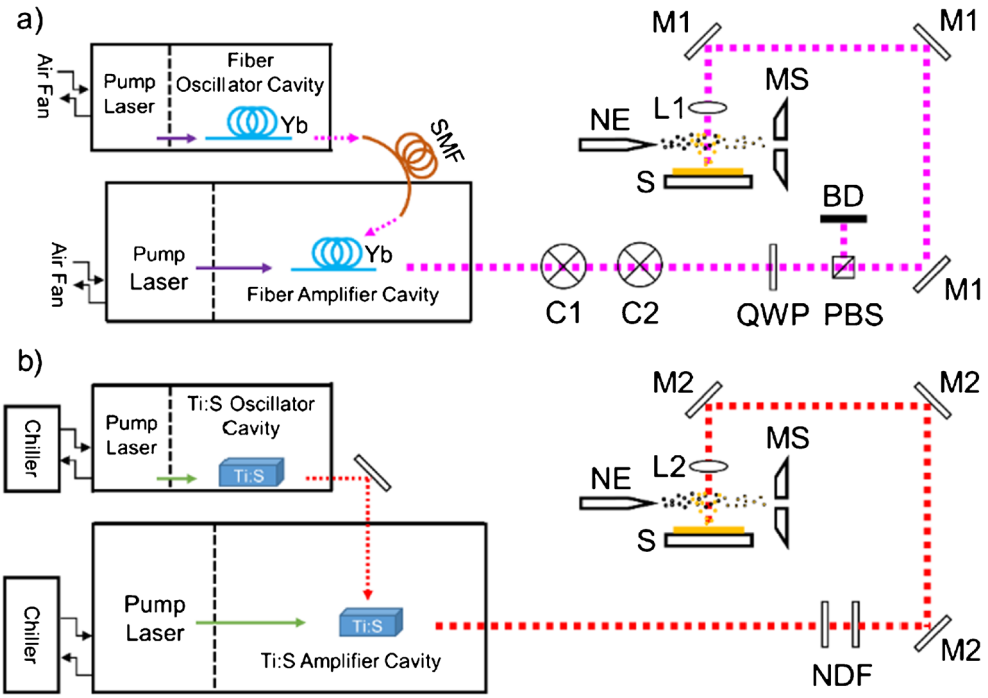

Figure 1. Schematic of **(a)** F-LEMS and **(b)** Ti:Sapphire-LEMS experimental setup. Yb, ytterbium-doped fiber; SMF, single-mode fiber; Ti:S, Ti:Sapphire crystal. M1, M2 are dielectric mirrors coated for 1042 nm and 800 nm wavelength, respectively. L1, L2 are 10 cm focal length lens coated for 1042 nm and 800 nm, respectively. C1, 20 Hz chopper; C2, 130 Hz chopper; QWP, quarter-wave plate; PBS, polarizing beam splitter cube; BD, beam dump; NDF neutral density filter; NE, nanospray emitter; S, metal sample stage; MS, mass spectrometer. Magenta and red dotted lines represent the 1042 nm and 800 nm laser beams whereas dark purple and green solid lines represent the pump laser beams in the corresponding laser systems. Note that the picture is not drawn to scale

All the assignments were further confirmed by comparing with literature data [12, 33, 39–50].

Results and Discussion

Direct Analysis of Plant Tissue by F-LEMS and Ti:Sapphire-LEMS Without Any Pretreatment

To compare the capabilities of the fiber and Ti:Sapphire femtosecond lasers for tissue sample analysis, fresh flower petals were affixed on the stainless steel substrates for analysis. The mass spectra acquired by F-LEMS and Ti:Sapphire-LEMS are shown in Figure 2a and b, respectively. The low-energy F-LEMS (46.5 μJ) mass spectrum displays a broad range of species, including anthocyanidin-associated flavonoid species. The features at *m/z* 581.2 and 727.2, corresponding to cyanidin-xylosyl-glucoside and cyanidin-xylosyl-rutinoside, and other anthocyanin features were observed as the dominant species from the flower petal, as listed in Table S-1 in the Supplementary Material. These anthocyanins were detected as preformed cations (see Supplementary Material Figure S-1) with modifications including derivatization of mono-glucosides, di-glucosides, acetyl-glucosides, and acetyl-rutinosides. Most of the peaks below *m/z* 200 are likely small organic acids, for example, 147.0 was assigned as coumaric acid with the loss of one water molecule, which are typically found as acyl functional groups for flavonoid species in the plant [33, 41]. Two features at *m/z* 867.2 and 1155.3, corresponding to singly protonated procyanidin oligomers with a degree of polymerization (DP) of 3 (DP3) and 4 (DP4) [42], were observed in the high mass region of the F-LEMS spectrum when magnified by 10. The high energy Ti:Sapphire-LEMS (280 μJ) spectrum displays the same molecular features with an additional feature of procyanidin DP5 at *m/z* 1443.3. Anthocyanins, one of the most common class of flavonoids, are naturally abundant pigments that help to protect the plant against excessive UV light radiation [51]. The detection of different anthocyanidins, anthocyanin glycosides, and procyanidin oligomers from the flower petals by F-LEMS and Ti:Sapphire-LEMS agrees with previous studies indicating that flavonoid species were abundant in plants using LC-ESI-MS [41, 52], atmospheric pressure MALDI-MS [53], as well as ambient ionization methods, including DESI-MS [54], ELDI-MS [52], and LAESI-MS [13, 40]. Note that further analysis with a separation step or CID and complementary fragmentation techniques are required to make definite assignment for the detected flavonoid ion species because of the presence of structural isomers [55].

To study the role of sample substrate on the laser vaporization of plant tissue by femtosecond laser pulses, flower petals

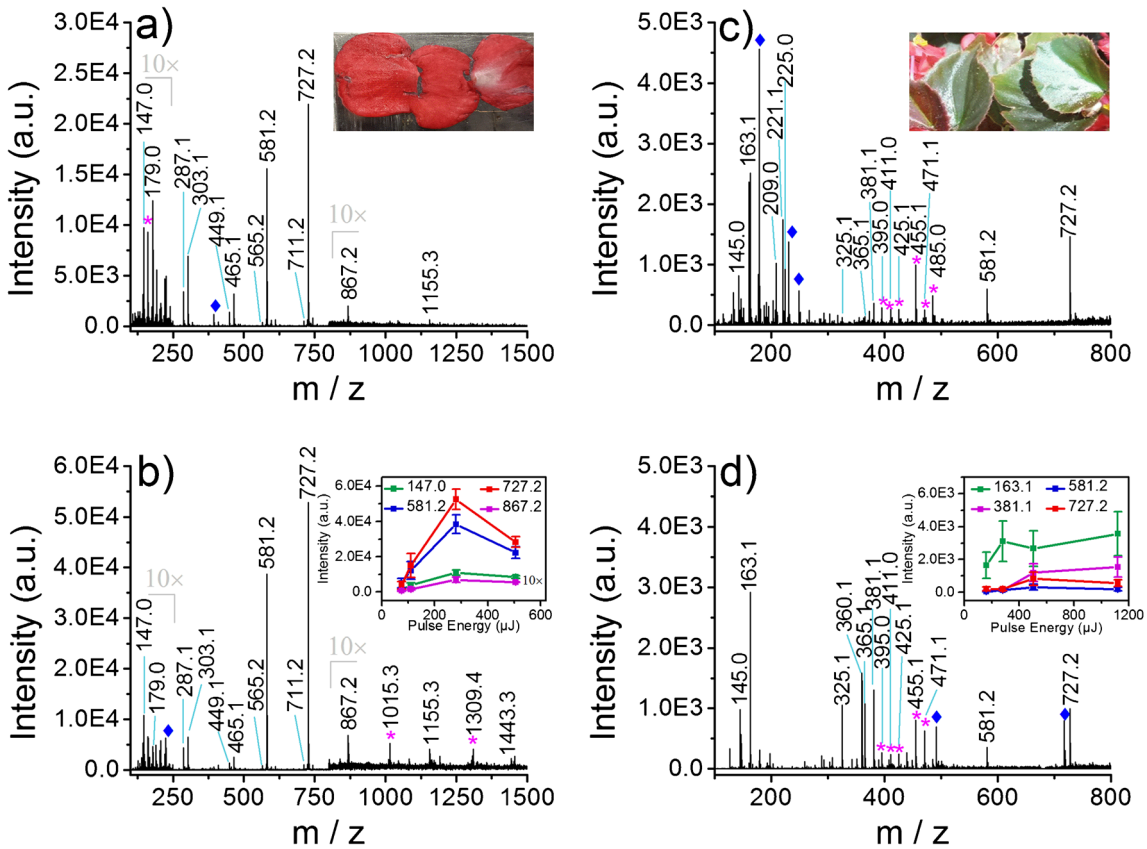

Figure 2. Blank-subtracted mass spectra for a flower petal affixed on a stainless steel substrate using **(a)** F-LEMS with 46.5 μJ pulse energy and **(b)** Ti:Sapphire-LEMS with 280 μJ pulse energy. Blank-subtracted mass spectra for a flower leaf affixed on a glass substrate using **(c)** F-LEMS with 46.5 μJ pulse energy and **(d)** Ti:Sapphire-LEMS with 505 μJ pulse energy. **Inset** of **(a)** and **(c)** display the photograph of the flower petal and leaf being analyzed by LEMS. **Inset** of **(b)** shows the intensity of representative ions (*m/z* 147.0, 581.2, 727.2, and 867.2) plotted as a function of pulse energy (75, 110, 280, and 500 μJ) for the flower petal using Ti:Sapphire-LEMS. **Inset** of **(d)** shows the intensity of representative ions (*m/z* 163.1, 381.1, 581.2, and 727.2) plotted as a function of pulse energy (160, 280, 500, and 1120 μJ) for the flower leaf using Ti:Sapphire-LEMS. Note that peaks labeled with ♦ and * are solvent and unidentified plant features, respectively

were analyzed on the glass substrates and compared with stainless steel substrates. Glass is a dielectric material that is transparent at the experimental near-IR laser wavelengths and is also a poor thermal conductor, and thus thermal desorption from the substrate was expected to be minimized. The spectra obtained by F-LEMS and Ti:Sapphire-LEMS laser vaporization displayed the same ion species, including the small metabolites and procyanidin trimer, and comparable ion intensities to results from stainless steel substrates, as seen in Supplementary Material Figure S-2. This suggests that a femtosecond laser pulse can interact with the plant materials directly via a nonresonant, multiphoton mechanism without sample substrate heating. Near-IR fs-LEMS is different from nanosecond UV and IR laser desorption techniques that require resonant absorption. For instance, direct analysis of secondary metabolites in plant tissues was enabled using matrix-free UV-laser desorption/ionization-MS at single-cell resolution because of a strong absorbance of UV light by the metabolites [56]. However, the results can be biased as many other plant metabolites are not strong UV-absorbers and their UV laser desorption probabilities can be limited. Universal interrogation of diverse metabolites from the plant sample has been illustrated by LAESI with 200 μm or higher spatial resolution because of the resonant absorption of the IR laser radiation by endogenous water matrix [13, 15].

Sample pretreatment (e.g., physical stripping [57], solvent extraction [54], or surface imprinting [58]) is sometimes required to remove the cuticular wax layers from the plant leaf surface for mass analysis when the penetration depth of the desorption probe is limited. Here, flower leaves were directly analyzed by the femtosecond laser pulses in the same manner as the flower petal without any pretreatment. The mass spectrum acquired using fiber laser vaporization followed by nanospray postionization (see Figure 2c) revealed similar features to the measurements of the high energy Ti:Sapphire laser, as shown in Figure 2d. A list of the assignments of molecular species from flower leaf by F-LEMS and Ti:Sapphire-LEMS analysis is provided in Supplementary Table S-2. Unlike flower petal, peaks at *m/z* 145.0 and

163.1, corresponding to protonated glucose with the loss of two and one water molecules, were observed as the dominant features in the leaf samples by F-LEMS and Ti:Sapphire-LEMS. Sucrose-related features at *m/z* 325.1, 365.1, and 381.1, corresponding to $[M - H_2O + H]^+$, $[M + Na]^+$ and $[M + K]^+$, were also found in the leaf samples by LEMS. The observation of these carbohydrates is expected as the leaf is the organ where photosynthesis takes place. The same anthocyanidin-related flavonoid features, namely cyanidin-xylosyl-glucoside (*m/z* 581.2) and cyanidin-xylosyl-rutinoside (*m/z* 727.2), were also observed from the leaf as the petal. The unique profile of metabolites in the plant, including flavonoids, carbohydrates, and other metabolites, can serve as signatures for rapid sample screening and classification, e.g., discriminating different varieties of grapes (Accent, Dunkelfelder, and Dakapo) [52], phenotypes of Impatiens flower petals [33], and color patterns of a Zebra plant leaf [34], using laser desorption followed by electrospray postionization MS techniques and multivariate statistical analysis.

The successful vaporization of plant tissue by the fiber laser radiation with <50 μJ pulses was unexpected at such low energy in comparison with the high energy Ti:Sapphire laser vaporization. To probe the effect of pulse energy for femtosecond laser vaporization, flower petals and leaves were analyzed by Ti:Sapphire-LEMS using pulse energies over an intensity range of nearly two orders of magnitude (μJ to mJ). Unfortunately, higher pulse energies (~mJ) are not currently available for the femtosecond fiber laser to perform a power study at higher energy range for F-LEMS. The mass spectra measured for a flower petal and a leaf at different laser pulse energies using Ti:Sapphire-LEMS are shown in the Supplementary Material Figure S-3 and Figure S-4, respectively. The intensity of representative peaks in the spectra of petal and leaf are plotted as a function of pulse energy and are displayed in the insets of Figure 2b and d. In the analysis of petals, peaks including *m/z* 581.2 and 727.2 increased significantly when the pulse energy was increased from 75 μJ to 505 μJ, where the maximum signal was observed at 280 μJ per pulse. The intensity of procyanidin oligomers also increased at much higher pulse energies (i.e., 280 and 505 μJ). Note that the spectra of flower petals by F-LEMS revealed comparable signal intensities for different glycosylated and polymerized anthocyanidins in comparison with the high energy Ti:Sapphire laser measurements. The comparable signal indicates that a femtosecond fiber laser with lower energy and longer wavelength is viable for laser vaporization in the analysis of plant materials. The analysis of leaf samples using Ti:Sapphire-LEMS also revealed higher ion yields at 505 and 1120 μJ, whereas negligible anthocyanin and sugar molecular features were observed at 160 μJ. This suggests that sufficiently high laser pulse energy is required to detect signal in agreement with previous Ti:Sapphire-LEMS and F-LEMS measurements of biological macromolecules [35]. The successful analysis of plant samples using fiber laser vaporization suggests that the low-energy laser vaporization is suitable for the direct analysis of complex biological systems.

Identification of A Lipid Standard by F-LEMS and Ti:Sapphire-LEMS Coupled with High Resolution/Accuracy Mass Spectrometer

Lipids play essential roles in cellular and tissue functions, including structure, energy storage, and signaling. Studies have shown that many human diseases (e.g., cancer, diabetes, and neurodegenerative diseases) involve the disruption of lipid metabolism and/or signaling [59]. An ambient ionization MS technique with the capability of rapid, spatially-resolved analysis for lipid detection is therefore of interest. An investigation of laser vaporization mass spectrometry of the lipid standard PC(6:0/6:0) was carried out to test the efficiency of femtosecond laser vaporization and nanospray postionization to transfer the lipid samples from the condensed phase to the gas phase for mass analysis. Previous analysis of PC(6:0/6:0) by Ti:Sapphire-LEMS using a pulse energy of 2.5 mJ revealed the detection of parent $[M + H]^+$ and fragment $[M - N(CH_3)_3 + Na]^+$ ions with the loss of trimethylamine end group [32]. The mass spectra of low-energy F-LEMS and Ti:Sapphire-LEMS are shown in Figure 3 with a peak at *m/z* 454.3 dominating the spectra, corresponding to protonated PC(6:0/6:0). Low abundance peaks at *m/z* 907.5 and 338.2, corresponding to a dimer ion $[2M + H]^+$ and a fragment ion $[M - C_6H_{12}O_2 + H]^+$ with the loss of one of the fatty acid chain, were observed in Ti:Sapphire-LEMS and were negligible in F-LEMS spectra. The analysis of the lipid by Ti:Sapphire-LEMS with much higher pulse energies at 280 and 505 μJ (see Supplementary Material Figure S-5a) show elevated intensity of fragment ions of *m/z* 338.2, as well as *m/z* 356.2 and 440.2, corresponding to $[M - C_6H_{12}O_2 + H_2O + H]^+$ and $[M - CH_2 + H]^+$, respectively. The survival yields calculated from the intensities of fragment and parent ions decreased from 0.93 to 0.80 with increasing pulse energy, as indicated in Supplementary Material Figure S-5c, presumably due to the more energetic excitation process under a higher intensity of a laser pulse. When the pulse energy was increased from 75 to 280 and 505 μJ, two species formed at *m/z* 468.2 and 486.3 via the intermolecular S_N2 transfer of a methyl group to a parent molecule to form $[M + CH_3]^+$ product and $[M + CH_3 + H_2O]^+$ water adduct ions as observed previously when the lipid cluster ions formed by ESI were subjected to collision-induced dissociation [60]. These measurements suggest that lipids can be desorbed intact from the substrates using low-energy femtosecond laser pulses.

High spectral resolution and accuracy-based mass measurements play an important role in unambiguous

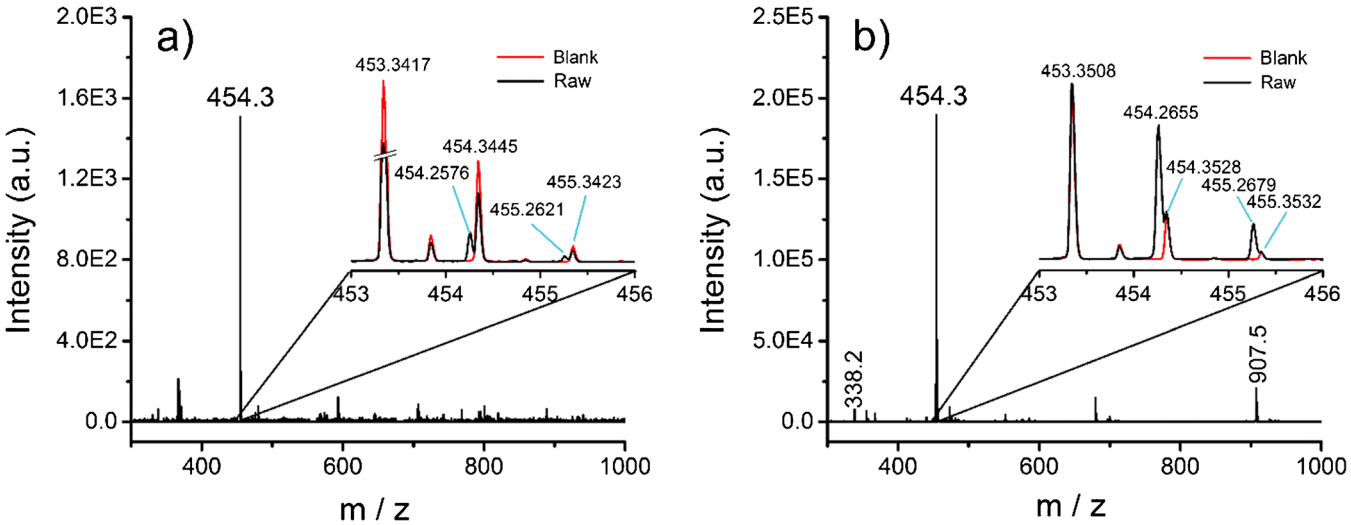

Figure 3. Blank-subtracted mass spectra for lipid standard PC(6:0/6:0) adsorbed on a stainless steel substrate using **(a)** F-LEMS with 46.5 μJ pulse energy and **(b)** Ti:Sapphire-LEMS with 75 μJ pulse energy. The **insets** show the expanded view of the PC(6:0/6:0) molecular ion peaks in the raw and blank spectra

identification of drugs, lipids, and metabolites species from tissue samples in mass spectrometry [10, 16]. We note that the high mass resolving power and accuracy of our QTOF analyzer enabled the identification of PC(6:0/6:0). The inset of Figure 3a demonstrates that the monoisotopic peak of PC(6:0/6:0) at *m/z* 454.2576 is resolved from one of the solvent-related blank features at *m/z* 454.3445 in the raw spectra, which would otherwise interfere with and/or obscure the lipid feature. The measured monoisotopic mass of PC(6:0/6:0) is also only 1.2 mDa difference from its theoretical value 454.2564. The lack of fragmentation for PC(6:0/6:0) using low-energy femtosecond laser pulses is an improvement to high energy Ti:Sapphire laser vaporization, which is beneficial for intact small molecule analysis by mass spectrometry.

Matrix-Free Analysis of A Mouse Brain Section by Ti:Sapphire-LEMS

Spatially-resolved ambient ionization MS analysis of animal tissue samples of histologic interest can directly provide chemical information to better understand the biological pathways and processes in the tissue. Molecular profiling and imaging of animal tissue samples with minimal sample preparation have been demonstrated by several ambient ionization MS techniques, including DESI [9, 25, 61], nano-DESI [10, 22], IR-MALDESI [11, 62], and LAESI [12, 63]. To investigate the possibility of using LEMS for the analysis of animal samples, mouse brain was chosen in our analysis. A freshly sectioned mouse brain was analyzed by Ti:Sapphire-LEMS without the deposition of external matrix, as seen in Figure 4. The mass spectrum revealed abundant ion features, especially at *m/z* 700–900 (Figure 4b). These features were identified as phospholipids, i.e., phosphatidylcholine (PC) and phosphatidylethanolamine (PE), and listed in Table S-3 in the Supplementary Material. The peak detected at *m/z* 760.6 corresponds to PC(34:1) and has been observed previously for the analysis of mouse brain section by MALDI [47–49], SIMS [45], and LAESI [12]. The low abundance features in the mass region *m/z* <700 are likely fragments of lipids or metabolites. For example, the peaks at *m/z* 551.5 and 577.5 have been suggested to arise from diacylglyceride molecules ($[M + H - H_2O]^+$) [64, 65] but could also be fragments of different classes of phospholipids with acyl chains of 32:0 and 34:1, respectively [66]. The ion at *m/z* 184.1 corresponds to either free phosphocholine molecules or phosphocholine fragments of PC lipids, which supports the detection of phosphatidylcholine species from the brain by LEMS. Further analysis by MS/MS or an ion mobility analyzer are required to confirm and elucidate the exact chemical structure of possible isobaric and/or isomeric ions because of the vast structural complexity and diversity of lipids [10, 63].

Section preparation is an important step in the analysis of animal tissue by mass spectrometry to ensure that sample integrity is maintained while avoiding sample contamination [67]. OCT-embedded mouse brain sections were analyzed by F-LEMS and Ti:Sapphire-LEMS to investigate the effect of the commonly employed embedding compounds in the process of cryosectioning on LEMS mass analysis. Figure S-6 in the Supplementary Material shows the spectra acquired from OCT-embedded brain samples using F-LEMS and Ti:Sapphire-LEMS. The lipids observed from fresh sectioned brain sample shown in Figure 4 were suppressed by species that are more readily ionized from the OCT compounds,

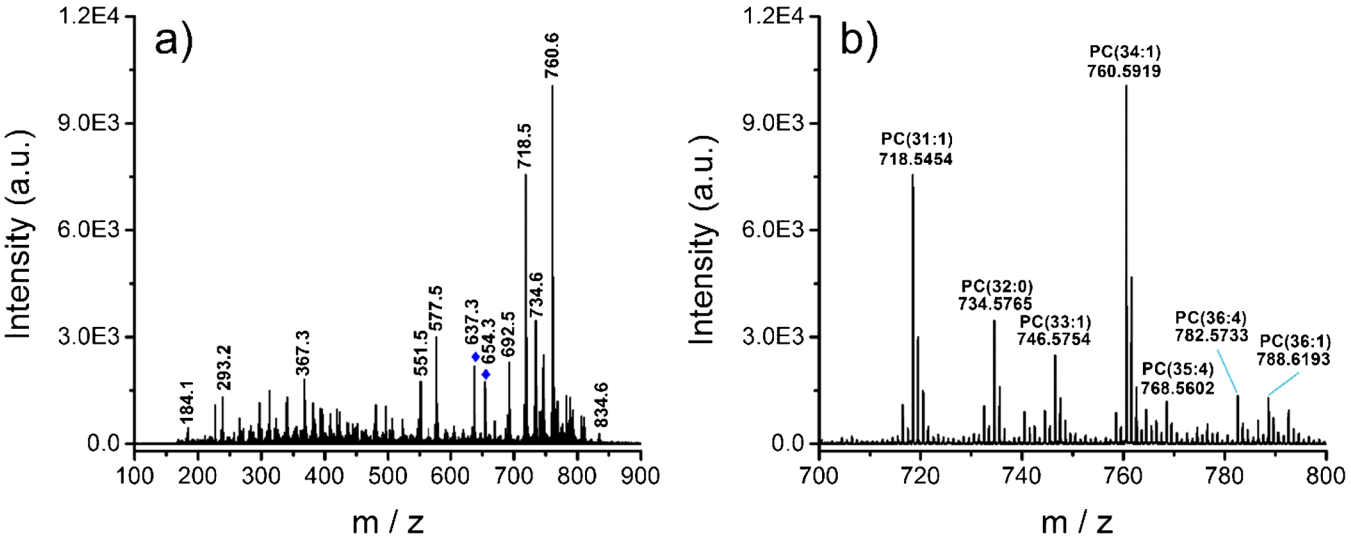

Figure 4. **(a)** Blank-subtracted mass spectrum for a coronal section of mouse brain tissue using Ti:Sapphire-LEMS with 280 μJ pulse energy. The *m/z* 700–900 region revealing the presence of various phospholipids is shown in **(b)**. Note that peaks labeled with ♦ are solvent features

including polyethylene glycol (PEG) and a possible polysaccharide with repeat units of 44 and 342 Da, respectively. This suggests that sample preparation is important to avoid ion suppression in the LEMS analysis of animal tissue samples. The OCT compound embedding process should be avoided; rather, flash freezing of the tissue block followed by cryosectioning to produce thin slices that are amenable to ambient ionization MS analysis [11, 12].

Conclusions

We demonstrated the use of a robust, turnkey femtosecond fiber laser to directly analyze tissue samples without the need for external matrix deposition. The results obtained with the low pulse energy (50 μJ) fiber laser source were comparable with analysis using a high energy Ti:Sapphire laser. The similarity of results with two different laser wavelengths suggests that femtosecond laser vaporization involves a nonresonant, multiphoton mechanism to enable universal analysis. Small metabolites, particularly anthocyanins, sugars, and their derivatives, were desorbed from plant samples. Various phospholipids were detected from mouse brain samples using femtosecond laser pulses from the Ti:Sapphire laser. The measurements are of interest for matrix-free mass analysis of tissue samples for the application of molecular imaging and tumor classification. The use of OCT compounds during tissue cryosectioning is detrimental for subsequent LEMS analysis.

The current study lays the groundwork for molecular imaging of plant and animal tissues using low-energy, femtosecond laser vaporization and electrospray postionization with minimal sample pretreatment. The femtosecond fiber laser has the advantage of being a turnkey, robust, and affordable laser that is amenable to non-specialist laboratories. With the rapid advances being make in fiber laser technology, the near-IR femtosecond laser desorption ambient ionization source may benefit from the development of femtosecond fiber lasers with milijoule pulse energy. MS/MS analysis such as collision induced dissociation may also be used in the future to validate the molecular assignments made by high spectral resolution and accuracy based mass measurements.

Acknowledgments

This work is supported by the National Science Foundation (CHE 0957694). The authors thank Dr. Teresa M. Reyes and Robert George (Perelman School of Medicine, University of Pennsylvania) for providing fresh mouse brain samples. The authors thank Dr. Yuri Persidsky (Department of Pathology and Laboratory Medicine, Temple University) for providing OCT cryosectioned mouse brain tissue section samples. The authors gratefully acknowledge laser support from Dr. Andrew Mills and Dr. Martin Fermann, and IMRA America, Inc.

References

1. Nicholson, J.K., Lindon, J.C.: Systems biology: metabonomics. Nature **455**, 1054–1056 (2008)
2. Svatoš, A.: Mass spectrometric imaging of small molecules. Trends Biotechnol. **28**, 425–434 (2010)
3. Baker, M.J., Trevisan, J., Bassan, P., Bhargava, R., Butler, H.J., Dorling, K.M., Fielden, P.R., Fogarty, S.W., Fullwood, N.J., Heys, K.A., Hughes, C., Lasch, P., Martin-Hirsch, P.L., Obinaju, B., Sockalingum, G.D., Sulé-Suso, J., Strong, R.J., Walsh, M.J., Wood, B.R., Gardner, P., Martin, F.L.: Using fourier transform IR spectroscopy to analyze biological materials. Nat. Protoc. **9**, 1771–1791 (2014)
4. Opilik, L., Schmid, T., Zenobi, R.: Modern Raman imaging: vibrational spectroscopy on the micrometer and nanometer scales. Annu. Rev. Anal. Chem. **6**, 379–398 (2013)

5. Monge, M.E., Harris, G.A., Dwivedi, P., Fernández, F.M.: Mass spectrometry: recent advances in direct open air surface sampling/ionization. Chem. Rev. **113**, 2269–2308 (2013)
6. So, P.-K., Hu, B., Yao, Z.-P.: Mass spectrometry: towards in vivo analysis of biological systems. Mol. BioSyst. **9**, 915–929 (2013)
7. Yew, J.Y., Cody, R.B., Kravitz, E.A.: Cuticular hydrocarbon analysis of an awake behaving fly using direct analysis in real-time time-of-flight mass spectrometry. Proc. Natl. Acad. Sci. U. S. A. **105**, 7135–7140 (2008)
8. Van Berkel, G.J., Kertesz, V., Koeplinger, K.A., Vavrek, M., Kong, A.-N.T.: Liquid microjunction surface sampling probe electrospray mass spectrometry for detection of drugs and metabolites in thin tissue sections. J. Mass Spectrom. **43**, 500–508 (2008)
9. Eberlin, L.S., Liu, X., Ferreira, C.R., Santagata, S., Agar, N.Y.R., Cooks, R.G.: Desorption electrospray ionization then MALDI mass spectrometry imaging of lipid and protein distributions in single tissue sections. Anal. Chem. **83**, 8366–8371 (2011)
10. Lanekoff, I., Burnum-Johnson, K., Thomas, M., Short, J., Carson, J.P., Cha, J., Dey, S.K., Yang, P., Prieto Conaway, M.C., Laskin, J.: High-speed tandem mass spectrometric in situ imaging by nanospray desorption electrospray ionization mass spectrometry. Anal. Chem. **85**, 9596–9603 (2013)
11. Robichaud, G., Barry, J.A., Garrard, K.P., Muddiman, D.C.: Infrared matrix-assisted laser desorption electrospray ionization (IR-MALDESI) imaging source coupled to a FT-ICR mass spectrometer. J. Am. Soc. Mass Spectrom. **24**, 92–100 (2013)
12. Nemes, P., Woods, A.S., Vertes, A.: Simultaneous imaging of small metabolites and lipids in rat brain tissues at atmospheric pressure by laser ablation electrospray ionization mass spectrometry. Anal. Chem. **82**, 982–988 (2010)
13. Nemes, P., Vertes, A.: Laser ablation electrospray ionization for atmospheric pressure, in vivo, and imaging mass spectrometry. Anal. Chem. **79**, 8098–8106 (2007)
14. Manicke, N.E., Yang, Q., Wang, H., Oradu, S., Ouyang, Z., Cooks, R.G.: Assessment of paper spray ionization for quantitation of pharmaceuticals in blood spots. Int. J. Mass Spectrom. **300**, 123–129 (2011)
15. Shrestha, B., Vertes, A.: In situ metabolic profiling of single cells by laser ablation electrospray ionization mass spectrometry. Anal. Chem. **81**, 8265–8271 (2009)
16. Pan, N., Rao, W., Kothapalli, N.R., Liu, R., Burgett, A.W.G., Yang, Z.: The Single-probe: a miniaturized multifunctional device for single cell mass spectrometry analysis. Anal. Chem. **86**, 9376–9380 (2014)
17. Harper, J.D., Charipar, N.A., Mulligan, C.C., Zhang, X., Cooks, R.G., Ouyang, Z.: Low-temperature plasma probe for ambient desorption ionization. Anal. Chem. **80**, 9097–9104 (2008)
18. Gross, J.H.: Direct analysis in real time—a critical review on DART-MS. Anal. Bioanal. Chem. **406**, 63–80 (2014)
19. Maldonado-Torres, M., López-Hernández, J.F., Jiménez-Sandoval, P., Winkler, R.: 'Plug and Play' assembly of a low-temperature plasma ionization mass spectrometry imaging (LTP-MSI) system. J. Proteome. **102**, 60–65 (2014)
20. Kertesz, V., Van Berkel, G.J.: Fully automated liquid extraction-based surface sampling and ionization using a chip-based robotic nanoelectrospray platform. J. Mass Spectrom. **45**, 252–260 (2010)
21. Roach, P.J., Laskin, J., Laskin, A.: Nanospray desorption electrospray ionization: an ambient method for liquid-extraction surface sampling in mass spectrometry. Analyst **135**, 2233–2236 (2010)
22. Laskin, J., Heath, B.S., Roach, P.J., Cazares, L., Semmes, O.J.: Tissue imaging using nanospray desorption electrospray ionization mass spectrometry. Anal. Chem. **84**, 141–148 (2012)
23. Watrous, J., Roach, P., Alexandrov, T., Heath, B.S., Yang, J.Y., Kersten, R.D., van der Voort, M., Pogliano, K., Gross, H., Raaijmakers, J.M., Moore, B.S., Laskin, J., Bandeira, N., Dorrestein, P.C.: Mass spectral molecular networking of living microbial colonies. Proc. Natl. Acad. Sci. U. S. A. **109**, E1743–E1752 (2012)
24. Takáts, Z., Wiseman, J.M., Gologan, B., Cooks, R.G.: Mass spectrometry sampling under ambient conditions with desorption electrospray ionization. Science **306**, 471–473 (2004)
25. Campbell, D., Ferreira, C., Eberlin, L., Cooks, R.G.: Improved spatial resolution in the imaging of biological tissue using desorption electrospray ionization. Anal. Bioanal. Chem. **404**, 389–398 (2012)
26. Flanigan, P.M., Levis, R.J.: Ambient femtosecond laser vaporization and nanosecond laser desorption electrospray ionization mass spectrometry. Annu. Rev. Anal. Chem. **7**, 229–256 (2014)
27. Shiea, J., Huang, M.-Z., Hsu, H.-J., Lee, C.-Y., Yuan, C.-H., Beech, I., Sunner, J.: Electrospray-assisted laser desorption/ionization mass spectrometry for direct ambient analysis of solids. Rapid Commun. Mass Spectrom. **19**, 3701–3704 (2005)
28. Sampson, J.S., Murray, K.K., Muddiman, D.C.: Intact and top-down characterization of biomolecules and direct analysis using infrared matrix-assisted laser desorption electrospray ionization coupled to FT-ICR mass spectrometry. J. Am. Soc. Mass Spectrom. **20**, 667–673 (2009)
29. Brady, J.J., Judge, E.J., Levis, R.J.: Mass spectrometry of intact neutral macromolecules using intense non-resonant femtosecond laser vaporization with electrospray post-ionization. Rapid Commun. Mass Spectrom. **23**, 3151–3157 (2009)
30. Judge, E.J., Brady, J.J., Dalton, D., Levis, R.J.: Analysis of pharmaceutical compounds from glass, fabric, steel, and wood surfaces at atmospheric pressure using spatially resolved, nonresonant femtosecond laser vaporization electrospray mass spectrometry. Anal. Chem. **82**, 3231–3238 (2010)
31. Judge, E.J., Brady, J.J., Levis, R.J.: Mass analysis of biological macromolecules at atmospheric pressure using nonresonant femtosecond laser vaporization and electrospray ionization. Anal. Chem. **82**, 10203–10207 (2010)
32. Brady, J.J., Judge, E.J., Levis, R.J.: Analysis of amphiphilic lipids and hydrophobic proteins using nonresonant femtosecond laser vaporization with electrospray post-Ionization. J. Am. Soc. Mass Spectrom. **22**, 762–772 (2011)
33. Flanigan, P.M., Radell, L.L., Brady, J.J., Levis, R.J.: Differentiation of eight phenotypes and discovery of potential biomarkers for a single plant organ class using laser electrospray mass spectrometry and multivariate statistical analysis. Anal. Chem. **84**, 6225–6232 (2012)
34. Judge, E.J., Brady, J.J., Barbano, P.E., Levis, R.J.: Nonresonant femtosecond laser vaporization with electrospray postionization for ex vivo plant tissue typing using compressive linear classification. Anal. Chem. **83**, 2145–2151 (2011)
35. Shi, F., Flanigan, P.M., Archer, J.J., Levis, R.J.: Direct analysis of intact biological macromolecules by low-energy, fiber-based femtosecond laser vaporization at 1042 nm wavelength with nanospray postionization mass spectrometry. Anal. Chem. **87**, 3187–3194 (2015)
36. Flanigan, P.M., Shi, F., Archer, J.J., Levis, R.J.: Internal energy deposition for low energy, femtosecond laser vaporization and nanospray post-ionization mass spectrometry using thermometer ions. J. Am. Soc. Mass Spectrom. **26**, 716–724 (2015)
37. Smith, C.A., O'Maille, G., Want, E.J., Qin, C., Trauger, S.A., Brandon, T.R., Custodio, D.E., Abagyan, R., Siuzdak, G.: METLIN—a metabolite mass spectral database. Ther. Drug Monit. **27**, 747–751 (2005)
38. Cotter, D., Maer, A., Guda, C., Saunders, B., Subramaniam, S.: LMPD: LIPID MAPS proteome database. Nucleic Acids Res. **34**, D507–D510 (2006)
39. Biesaga, M., Pyrzynska, K.: Liquid chromatography/tandem mass spectrometry studies of the phenolic compounds in honey. J. Chromatogr. A **1216**, 6620–6626 (2009)
40. Nemes, P., Barton, A.A., Li, Y., Vertes, A.: Ambient molecular imaging and depth profiling of live tissue by infrared laser ablation electrospray ionization mass spectrometry. Anal. Chem. **80**, 4575–4582 (2008)
41. Giusti, M.M., Rodríguez-Saona, L.E., Griffin, D., Wrolstad, R.E.: Electrospray and tandem mass spectroscopy as tools for anthocyanin characterization. J. Agric. Food Chem. **47**, 4657–4664 (1999)
42. Ohnishi-Kameyama, M., Yanagida, A., Kanda, T., Nagata, T.: Identification of catechin oligomers from apple (Malus pumila cv. Fuji) in matrix-assisted laser desorption/ionization time-of-flight mass spectrometry and fast-atom bombardment mass spectrometry. Rapid Commun. Mass Spectrom. **11**, 31–36 (1997)
43. Coello, Y., Jones, A.D., Gunaratne, T.C., Dantus, M.: Atmospheric pressure femtosecond laser imaging mass spectrometry. Anal. Chem. **82**, 2753–2758 (2010)
44. Xin, G.-Z., Hu, B., Shi, Z.-Q., Lam, Y.C., Dong, T.T.-X., Li, P., Yao, Z.-P., Tsim, K.W.K.: Rapid identification of plant materials by wooden-tip electrospray ionization mass spectrometry and a strategy to differentiate the bulbs of Fritillaria. Anal. Chim. Acta **820**, 84–91 (2014)
45. Passarelli, M.K., Winograd, N.: Lipid imaging with time-of-flight secondary ion mass spectrometry (ToF-SIMS). Biochim. Biophys. Acta Mol. Cell Biol. Lipids **1811**, 976–990 (2011)
46. Shrestha, B., Nemes, P., Nazarian, J., Hathout, Y., Hoffman, E.P., Vertes, A.: Direct analysis of lipids and small metabolites in mouse brain tissue by AP IR-MALDI and reactive LAESI mass spectrometry. Analyst **135**, 751–758 (2010)

47. Meriaux, C., Franck, J., Wisztorski, M., Salzet, M., Fournier, I.: Liquid ionic matrixes for MALDI mass spectrometry imaging of lipids. J. Proteome. **73**, 1204–1218 (2010)
48. Matusch, A., Fenn, L.S., Depboylu, C., Klietz, M., Strohmer, S., McLean, J.A., Becker, J.S.: Combined elemental and biomolecular mass spectrometry imaging for probing the inventory of tissue at a micrometer scale. Anal. Chem. **84**, 3170–3178 (2012)
49. Thomas, A., Charbonneau, J.L., Fournaise, E., Chaurand, P.: Sublimation of new matrix candidates for high spatial resolution imaging mass spectrometry of lipids: enhanced information in both positive and negative polarities after 1,5-diaminonapthalene deposition. Anal. Chem. **84**, 2048–2054 (2012)
50. Delvolve, A.M., Colsch, B., Woods, A.S.: Highlighting anatomical substructures in rat brain tissue using lipid imaging. Anal. Methods **3**, 1729–1736 (2011)
51. Castañeda-Ovando, A., Pacheco-Hernández, M.L., Páez-Hernández, M.E., Rodríguez, J.A., Galán-Vidal, C.A.: Chemical studies of anthocyanins: a review. Food Chem. **113**, 859–871 (2009)
52. Berisha, A., Dold, S., Guenther, S., Desbenoit, N., Takats, Z., Spengler, B., Römpp, A.: A comprehensive high-resolution mass spectrometry approach for characterization of metabolites by combination of ambient ionization, chromatography, and imaging methods. Rapid Commun. Mass Spectrom. **28**, 1779–1791 (2014)
53. Li, Y., Shrestha, B., Vertes, A.: Atmospheric pressure infrared MALDI imaging mass spectrometry for plant metabolomics. Anal. Chem. **80**, 407–420 (2008)
54. Li, B., Hansen, S.H., Janfelt, C.: Direct imaging of plant metabolites in leaves and petals by desorption electrospray ionization mass spectrometry. Int. J. Mass Spectrom. **348**, 15–22 (2013)
55. Abrankó, L., Szilvássy, B.: Mass spectrometric profiling of flavonoid glycoconjugates possessing isomeric aglycones. J. Mass Spectrom. **50**, 71–80 (2015)
56. Hölscher, D., Shroff, R., Knop, K., Gottschaldt, M., Crecelius, A., Schneider, B., Heckel, D.G., Schubert, U.S., Svatoš, A.: Matrix-free UV-laser desorption/ionization (LDI) mass spectrometric imaging at the single-cell level: distribution of secondary metabolites of Arabidopsis thaliana and Hypericum species. Plant J. **60**, 907–918 (2009)
57. Li, B., Bjarnholt, N., Hansen, S.H., Janfelt, C.: Characterization of barley leaf tissue using direct and indirect desorption electrospray ionization imaging mass spectrometry. J. Mass Spectrom. **46**, 1241–1246 (2011)
58. Müller, T., Oradu, S., Ifa, D.R., Cooks, R.G., Kräutler, B.: Direct plant tissue analysis and imprint imaging by desorption electrospray ionization mass spectrometry. Anal. Chem. **83**, 5754–5761 (2011)
59. Gode, D., Volmer, D.A.: Lipid imaging by mass spectrometry—a review. Analyst **138**, 1289–1315 (2013)
60. James, P.F., Perugini, M.A., O'Hair, R.A.J.: Sources of artefacts in the electrospray ionization mass spectra of saturated diacylglycerophosphocholines: from condensed phase hydrolysis reactions through to gas phase intercluster reactions. J. Am. Soc. Mass Spectrom. **17**, 384–394 (2006)
61. Eberlin, L.S., Gabay, M., Fan, A.C., Gouw, A.M., Tibshirani, R.J., Felsher, D.W., Zare, R.N.: Alteration of the lipid profile in lymphomas induced by MYC overexpression. Proc. Natl. Acad. Sci. U. S. A. **111**, 10450–10455 (2014)
62. Barry, J.A., Groseclose, M.R., Robichaud, G., Castellino, S., Muddiman, D.C.: Assessing drug and metabolite detection in liver tissue by UV-MALDI and IR-MALDESI mass spectrometry imaging coupled to FT-ICR MS. Int. J. Mass Spectrom. **377**, 448–455 (2014)
63. Shrestha, B., Vertes, A.: High-throughput cell and tissue analysis with enhanced molecular coverage by laser ablation electrospray ionization mass spectrometry using ion mobility separation. Anal. Chem. **86**, 4308–4315 (2014)
64. Altelaar, A.F.M., Klinkert, I., Jalink, K., de Lange, R.P.J., Adan, R.A.H., Heeren, R.M.A., Piersma, S.R.: Gold-enhanced biomolecular surface imaging of cells and tissue by SIMS and MALDI mass spectrometry. Anal. Chem. **78**, 734–742 (2005)
65. Magnusson, Y.K., Friberg, P., Sjövall, P., Malm, J., Chen, Y.: TOF-SIMS analysis of lipid accumulation in the skeletal muscle of ob/ob mice. Obesity **16**, 2745–2753 (2008)
66. Pulfer, M., Murphy, R.C.: Electrospray mass spectrometry of phospholipids. Mass Spectrom. Rev. **22**, 332–364 (2003)
67. Schwartz, S.A., Reyzer, M.L., Caprioli, R.M.: Direct tissue analysis using matrix-assisted laser desorption/ionization mass spectrometry: practical aspects of sample preparation. J. Mass Spectrom. **38**, 699–708 (2003)